Statistics and scarring of eigenvectors of a shell model

D. C. Meredith
Physics Department, University of New Hampshire, Durham, New Hampshire 03824
(Received 18 August 1992)

We examine the eigenvector component statistics for a quantum system whose classical analog exhibits chaos. Combining the unfolded components from all eigenvectors to achieve high statistics, we are able to compare random-matrix theory and numerical experiment in detail by fitting the data to a χ^2 distribution with ν degrees of freedom. Although there are statistically significant deviations between the fit and data, component fluctuations are shown to be well modeled by Gaussian-orthogonal-ensemble fluctuations. By examining the component statistics of the scarred eigenvectors alone, we find that they are also in qualitative agreement with random-matrix theory, giving evidence that scarring by periodic orbits and statistics of fluctuations are compatible features of the eigenstates.

PACS number(s): 05.45.+b, 03.65.Sq, 03.65.Ge

I. INTRODUCTION

Semiclassical methods are an invaluable tool in the study of quantum systems. Not only are they often much simpler than the full quantum calculation, but they also exploit our classical intuition, the value of which cannot be overestimated. Unfortunately, the most well-known semiclassical methods (Bohr-Sommerfeld, WKB, and Einstein-Brillouin-Keller [1]) are only appropriate when the classical limit is integrable (i.e., the number of constants of the motion is equal to the number of degrees of freedom [2]), yet these are a set of measure zero in the space of Hamiltonians [3]. To remedy this situation, other theoretical methods are being explored that are appropriate for generic Hamiltonian systems.

Two very different methods are of interest in this paper. The first is periodic-orbit theory (POT) based on the work of Gutzwiller [4], and Balian and Block [5]. POT derives classical formulas (i.e., formulas using only classical quantities) for quantum-mechanical objects: the density of states, energy-smoothed Wigner function [6], and energy- and space-smoothed eigenfunctions in coordinate space [7]. These formulas begin with the Van Vleck time propagator [4,8] and use successive stationary phase integrations (appropriate as $\hbar \to 0$) to derive the quantities of interest. In each case, the final expression has a smooth term and an oscillatory term with a contribution from each periodic orbit of the system. This approach has given us the marvelous insight that short periodic orbits have great influence on the quantum system. A striking influence of periodic orbits is seen in the scarring of eigenstates, which was first understood by Heller [9] using the time evolution of wave packets. Scarred states are those which have an unexpectedly high probability density in the vicinity of a periodic orbit. In related work by Du and Delos [10], we see that the oscillations in an absorption spectrum of a hydrogen atom are due to the presence of short, closed orbits in the classical analog.

The origins and philosophy of random-matrix theory (RMT) [11,12] are completely different: RMT was motivated by the need of nuclear physicists to understand the details of highly excited nuclear levels. The philosophy is borrowed from statistical mechanics: if our Hamiltonian is a typical member of an ensemble of random Hamiltonians (i.e., random Hermitian matrices) and the ensemble is ergodic (i.e., averages over the eigenvalues of a single member are equivalent to averages over the ensemble), then the (hopefully calculable) ensemble averages can be substituted for (practically incalculable) energy averages. Several ensembles were proposed, some for their physical plausibility, some for their mathematical tractability. The Gaussian orthogonal ensemble (GOE) gained prominence because ensemble averages could be calculated [12–15]. However, it was not at all clear that any Hamiltonian of a real physical system was a typical member of such a simple ensemble. Therefore this approach, begun in the 1950s, was revitalized in the early 1980s when Haq, Pandey, and Bohigas [16, 17] demonstrated that the fluctuations of real nuclear levels share the statistical properties of the GOE.

RMT was introduced into quantum chaology soon after by Bohigas, Giannoni, and Schmit [18], who studied the statistics of fluctuations (about the smooth background) of the spectrum of the (classically chaotic) stadium and Sinai's billiards. They found that these fluctuations were also in agreement with the statistical fluctuations of the GOE, even though these system had only two degrees of freedom while the nuclear data came from much more complicated systems. They conjectured that any system whose classical analog is chaotic will show GOE statistical fluctuations. There has been much evidence that this is the case, with most work focusing on the eigenvalues statistics [19]. The most astounding feature of these results is that the statistical properties of the fluctuations are universal, depending only on the general nature of the dynamics (regular versus chaotic) and indifferent to the details of the dynamics.

Although these two theories differ greatly in their approach, their conclusions are not without agreement. In

particular, Berry [20] was able to show that the Δ_3 statistic, which measures the long-range order, is the same for both POT and RMT for short energy intervals. However, Berry goes on to show that this agreement between the two approaches is destroyed by the presence of a shortest periodic orbit (with period $T_{\min}$): when $\Delta E \approx \hbar/T_{\min}$ periodic-orbit theory predicts a saturation of the statistic while random-matrix theory predicts no saturation. This saturation has been confirmed in numerical data from many different systems [19]. The lesson learned is that the universality of random-matrix theory holds when the statistic in question is supported by the contribution of many long periodic orbits, but when short (and very particular) periodic orbits dominate, RMT fails.

In this paper we will explore the eigenvector statistics in more detail, including stricter goodness of fit tests on the data than have been done previously. But more importantly, we will explore the interplay between the universal statistics and the particular short periodic orbits. We will show that for the eigenvectors, the presence of scarring by the short periodic orbits does not destroy the universality of the statistics. We will also investigate the sharing of scar strength among eigenstates.

We begin in Sec. II with a review of results for eigenvector statistics from RMT as well as the extensions to that theory; Sec. III summarizes the work done by others; Sec. IV introduces the shell model; Sec. V discusses our procedures in detail; and our results are given in Sec. VI.

II. COMPONENT STATISTICS: THEORY

In order to understand the eigenvector component distribution, it is essential to understand the information content of the GOE: it is the least biased distribution of Hamiltonians, given only the constraints that there is a limit on the size of the matrix elements, and that the probability distribution is normalizable [21]. The form of the distribution is obtained by maximizing the entropy,

$$I \equiv -\int P(H)\ln[P(H)]dH \tag{1}$$

(i.e., minimizing the bias), subject to the above constraints. The resulting distribution for the matrix elements shows that they are independent and Gaussian distributed if the original matrix is real and symmetric. As is expected on physical grounds, the resulting distribution is invariant under orthogonal transformations.

The distribution of the matrix elements can be changed into a distribution for eigenvalues and eigenvectors. However, the joint eigenvector component distribution is obtained more hueristically by noting the following: since the distribution is invariant under orthogonal transformations, all normalized eigenvectors are equally probable. The resulting joint probability for the components $x_{i\lambda} \equiv \langle i|\lambda\rangle$ (where i denotes a basis state and λ denotes an eigenstate) of one eigenvector is as follows:

$$P_{\text{joint}}(x_{1\lambda}, x_{2\lambda}, \ldots, x_{\mathcal{N}\lambda}) = \text{const} \times \delta\left[\sum_{i=1}^{\mathcal{N}} x_{i\lambda}^2 - 1\right] . \tag{2}$$

The probability for an individual component of a single eigenvector can be derived by integrating over all but one component ($x \equiv x_{i_0\lambda}$) [14]:

$$P_{\text{finite}}(x) = \frac{1}{\sqrt{\pi}}\Gamma\left(\frac{\mathcal{N}}{2}\right)\Gamma\left(\frac{\mathcal{N}-1}{2}\right)(1-x^2)^{(\mathcal{N}-3)/2} . \tag{3}$$

The GOE result is the result in the limit of large matrices:

$$P_{\text{GOE}}(x) \equiv \lim_{\mathcal{N}\to\infty} P_{\text{finite}}(x) = \left(\frac{\mathcal{N}}{2\pi}\right)^{1/2}\exp(-x^2\mathcal{N}/2) . \tag{4}$$

The Porter-Thomas (PT) distribution is the corresponding distribution for the square of the component $y = x^2$:

$$P_{\text{PT}}(y) = \left(\frac{1}{2\langle y\rangle}\right)^{1/2}\frac{y^{-1/2}\exp(-y/2\langle y\rangle)}{\Gamma(1/2)} , \tag{5}$$

where $\langle y\rangle = 1/\mathcal{N}$ is the energy averaged value of y.

One objection to looking for universality in eigenvector statistics is that any calculations with eigenvectors must be basis dependent. This objection is overcome by first unfolding the components, i.e., by dividing the $y_{i,\lambda}$ for a given basis state by the local energy average value [14]:

$$\langle y_i[E = (E_{\lambda_2} - E_{\lambda_1})/2]\rangle \equiv \sum_{\lambda=\lambda_1}^{\lambda_2} y_{i,\lambda} \tag{6}$$

where the energy range between E_{λ_1} and E_{λ_2} is quantum-mechanically large (i.e., there are many eigenstates) but classically small (i.e., the classical dynamics do not vary significantly in that range). In this way the statistics are describing fluctuations from the local energy averaged value, and not the values themselves. Note that unfolding must also be done for the eigenvalues [12–14]. Therefore the only inappropriate bases are those for which such unfolding cannot be done. To take an extreme example, the basis of the eigenvectors themselves is inappropriate since the overlap of the eigenvectors with each other is not a smooth function of energy.

One limitation of the GOE prediction is that it applies only to systems whose classical analog is chaotic, yet many systems have classical dynamics that is regular in some regions of the energy shell and chaotic in others. For such systems, the work of Alhassid, Feingold, and Levine extends the results of RMT [22, 23] by investigating a component distribution with a variable shape. The distribution was derived by the maximum-entropy method as described above, with the additional constraint on the deviations of y from $\langle y\rangle$. The resulting distribution is the χ^2 probability distribution for ν degrees of freedom:

$$P_\nu(y) = B\left(\frac{\nu}{2\langle y\rangle}\right)^{\nu/2}\frac{y^{\nu/2-1}\exp(-\nu y/2\langle y\rangle)}{\Gamma(\nu/2)} . \tag{7}$$

(The value of B should be one for correct normalization. However, we will fit the data to find the best value of B.) The Porter-Thomas distribution corresponds to $\nu = 1$.

As ν decreases to zero the number of very small components and very large components increases—exactly what we would expect in the regular region where there are more constraints on the eigenvectors. Although they do not propose that this must be the distribution as the degree of regularity increases, they suggest that it will follow the expected trends and, through the value of ν, give a quantitative description of the degree of randomness or order in the eigenstates.

One final consideration is the correlations between eigenvector components. We know that these must be correlated because of the normalization constraint. However, Brody *et al.* [14] show that n of these are independent if $(\mathcal{N}-n) \gg 1$, where $\mathcal{N}$ is the basis size. In addition, the correlations between eigenvector components of different eigenstates decay as $1/(\mathcal{N}-1)^2$.

III. COMPONENT STATISTICS: PREVIOUS RESULTS

Although eigenvalue statistics have been much more intensely studied, there are many results on eigenvector statistics as well. Much of the early work was done on nuclear systems, focusing on reduced widths and transition matrix elements, which are also expected to follow the Porter-Thomas distribution [14]. Good agreement with this expectation was found in experimental neutron resonance width fluctuations by Liou *et al.* [24], in reduced widths for proton resonance in the compound nuclei by Mitchell *et al.* [25], in numerically determined transitions between two shell model bases by Draayer, French, and Wong [26], and by many others [27]. Alhassid, Novoselsky, and Whelan [28] have examined the eigenvalue and transition-matrix-element statistics in the interacting-boson model for a large range of parameters and found (by comparison with classical Lyapunov exponents, the rate of exponential divergence of trajectories) that both eigenvector and eigenvalue statistics were correlated with the degree of chaos in the classical limit.

The prediction of eigenvector statistics has also been tested in several two-degree-of freedom chaotic systems. Much of this work was inspired by Berry's conjecture that $\Psi(x,y)$ for a chaotic system should be a Gaussian random function of position [1]. The conjecture comes from the realization that a chaotic wave function is a random superposition of waves with all possible directions, and so must be a random state. This is in contrast to the eigenstates of an integrable system which are a superposition of only a finite number of waves. Note that Berry's conjecture is precisely the GOE result when the basis states are the eigenstates of position. It is also important to note that in the case of two-degree-of-freedom Hamiltonians of the kinetic plus potential type, each region of coordinate space that is energetically accessible is equally accessible [1]; hence in all of the following systems no unfolding of the components was necessary.

In all systems studied, general agreement has been found with Berry's prediction. Sinai's billiard with a point scatterer has been studied by Šeba [29]; this is a system which is pseudointegrable yet the eigenvalue and eigenvector statistics match those of the GOE. The wave functions of the chaotic stadium billiard have been studied by MacDonald and Kaufman [30] and Shapiro and Goelman [31]; both groups found agreement with Berry's conjecture. As one exception, MacDonald and Kaufman found that states clearly scarred by bouncing ball modes (i.e., an unusual case of marginally stable, nonisolated periodic orbits) did not follow the Porter-Thomas prediction. The quasienergy eigenstates of the kicked rotor (a chaotic time-dependent system) have been examined by Israliev [32], who found that their statistics were fit with a high confidence level by the finite $\mathcal{N}$ formula ($\mathcal{N}$=99) given by Eq. (3). The quantal problem for a free particle on a surface of constant negative curvature (whose classical motion is ergodic) was studied by Aurich and Steiner [33], who found the expected Gaussian random behavior. They also raised a question which we would like to take up: Are scars and Gaussian random behavior compatible?

IV. MODEL

The system that we explore is the Lipkin-Meshkov-Glick model [34]. This is a quasispin system with its origins in nuclear structure physics. The model consists of M interacting nucleons in three M-fold degenerate levels. Because of the degeneracy there is no Pauli blocking. This Hamiltonian can be written in terms of the generators G_{ij} of a u(3) algebra [35]

$$H = \sum_{\substack{i,j=0 \\ (i \neq j)}}^{2} G_{ij}^2 , \tag{8}$$

where

$$G_{ij} = \sum_{m=1}^{M} a_{im}^{\dagger} a_{jm}, \quad G_{ij}^{\dagger} = G_{ji}, \quad i,j = 0,1,2 \tag{9}$$

and $(a_{im}^{\dagger},\ a_{im})$ are the usual creation-annihilation fermionic operators. The labels i and $j = 0, 1$, or 2 indicate the ground, first, or second single-particle level, while m labels the particle number. The conservation of the total number of particles introduces a new constraint and consequently the dynamical group is the SU(3) group.

The Hamiltonian is symmetric under particle interchange, so we may solve the eigenvalue equation in the subbasis which is completely symmetric under particle interchange. This basis is labeled by only two numbers: the population in levels zero and one, with the population in level two fixed by number conservation. This choice of basis will lead to a classical limit with only two degrees of freedom (see below).

The Hamiltonian is also symmetric under level interchange and conserves the evenness or oddness of the population of each level. If we fix the population of the ground level to be even, and the population of the other two levels to be odd, then the symmetries allow us to label the basis states by m_0 (the number of particles in the ground state) and $\Delta m_{12} \equiv |m_1 - m_2|$ (the difference between the number of particles in the two excited states). With these choices of symmetry classes and $M = 120$, the total number of eigenvalues is 930. (Details of the

quantum problem can be found in an earlier paper [36].)

The classical limit is obtained in the limit that $M \to \infty$. Intuitively, in this limit the system becomes macroscopic and should behave classically. Rigorously, the classical Hamiltonian is the expectation value of H/M in a coherent state [37–39]. For the Lipkin model, the Hamiltonian may be written as follows:

$$\mathcal{H}(\mathbf{I},\theta) = I_0 I_2 \cos[2(\theta_2 - \theta_0)] + I_1 I_0 \cos[2(\theta_0 - \theta_1)] + I_1 I_2 \cos[2(\theta_2 - \theta_1)] , \quad (10)$$

where the action variables (I_0, I_1, I_2) are the classical continuous analogs of the shell occupation numbers (m_0, m_1, m_2) (scaled by M) and satisfy the conditions

$$0 \le I_i \le 1 , \qquad i = 0,1,2 \quad (11)$$

$$I_0 + I_1 + I_2 = 1 . \quad (12)$$

(This system appears to have three degrees of freedom; however, if we take into account $I_0 + I_1 + I_2 = 1$ and define the angles $\phi_i = \theta_i - \theta_0$, $i = 1,2$, it is clear that there are only two degrees of freedom.) Because of the constraints on I_i and the periodicity of θ, the phase space is a compact four-sphere. The action space $I_1 - I_2$ is a triangle with vertices at $(0,0), (1,0)$, and $(0,1)$.

Details of the classical limit appear in earlier papers [36, 38, 39]. Of particular interest here is the degree of chaos as determined by the chaotic volume (i.e., the fraction of phase space with positive Lyapunov exponents) [36]. The dynamics is judged chaotic for $0.0162 < E < 0.242$, quasichaotic for $-0.149 < E < 0.0162$, and regular for $-0.25 < E < -0.149$ and $0.242 < E < 0.333$. Only in the chaotic regime is the chaotic volume relatively constant for the whole energy range; for the other two classes, the degree of chaos varies. In analyzing the eigenvectors, we will separate the states into the three dynamics classes (chaotic, quasichaotic, and regular) based on their eigenvalue and the above energy ranges.

In this paper we study the effect of scarring by periodic orbits on the statistics of the eigenstates. The scarring has been studied in detail in a previous paper [40]. This model has three families of periodic orbits which are confined to a line at the edge of the action triangle; this simple geometry makes them relatively easy to analyze. The families are defined by $I_i = 0$ for $i = 0, 1$, or 2. A quick examination of Hamilton's equations for this system show that if any action is zero for any time, then it is zero for all times. Therefore along an $I_i = 0$ line, one of the actions drops out of Eq. (10), and the Hamiltonian reduces to a one degree of freedom system. The resulting motion must be periodic since all orbits lie on one-dimensional tori, i.e., topological circles. These are short, slightly unstable periodic orbits which scar the eigenvectors.

V. PROCEDURE

The quantity of interest in this paper is the square of the eigenvector components in the basis labeled by the populations of the levels:

$$y(m_0, \Delta m_{12}, \mu) \equiv \langle m_0, \Delta m_{12} | \mu \rangle^2 . \quad (13)$$

The general procedure is to unfold the components, histogram the components (for a fixed basis state or eigenstate), and then fit the histogram to a probability distribution.

The first step in unfolding the components is to find the local energy averaged value of a fixed components (fixed m_0 and Δm_{12}) as given by Eq. (6). However, we do not have enough quantum levels to have an energy region that is both quantum-mechanically large and classically small. Instead, the average was found by smoothing the data with a Gaussian weighting factor:

$$y_{\rm av}(m_0, \Delta m_{12}, E_\lambda; \gamma) \equiv \frac{\sum_{\mu=1}^{\mathcal{N}} y(m_0, \Delta m_{12}, \mu) \exp(-[E_\lambda - E_\mu]^2/[2\gamma^2])}{\sum_{\mu=1}^{\mathcal{N}} \exp(-[E_\lambda - E_\mu]^2/[2\gamma^2])} ; \quad (14)$$

the normalization factor in the denominator was chosen so that $\sum_{m_0, \Delta m_{12}} y_{\rm av} = 1$. The smoothing cannot be done accurately at the ends of the spectrum, so these components are left out of the analysis; the number left out depends upon the choice of γ.

The fluctuations of the components about the average value are precisely the unfolded components:

$$\xi(m_0, \Delta m_{12}, \lambda, \gamma) \equiv \frac{y(m_0, \Delta m_{12}, \lambda)}{y_{\rm av}(m_0, \Delta m_{12}, E_\lambda; \gamma)} . \quad (15)$$

Because of the unfolding, the value of $\langle \xi \rangle$ averaged over energy (i.e., λ) should be one; for most cases it was greater than 0.9.

However, for some basis vectors the energy average was much smaller (as small as 0.2) indicating that the desired unfolding could not be accomplished by the Gaussian smoothing. These basis vectors which give rise to these low values of $\langle \xi \rangle$ are quasieigenvectors of the problem. To see this, note that the corners of the $I_1 - I_2$ triangle are classically energetically accessible only at $E = 0$; therefore there is little quantum probability to be in the corners at other energies; the components drop off exponentially as the energy eigenvalue moves away from zero. Because of the strong energy dependence, the simple Gaussian smoothing does not correctly unfold the components. (Note that the unfolding for all states could be done in principle, but it is difficult to unfold all components automatically, since the energy dependence can vary greatly from component to component.) In all further analysis, the components with $\langle \xi \rangle$ less than 0.85 are not included. (The motivation for this value of the cutoff will be explained in the section on scarred states.) These corner states account for 16% of the basis states. The unfolding and discarding of corner basis states was not done in previous work [36], hence we do not expect agreement with those results.

The ξ values depend on the choice of the smoothing parameter γ. We chose γ based on Berry's separation of energy scales [20]. $E_{\rm min}$ is the inner energy scale which is equivalent to the average energy spacing. Once the eigenvalues are unfolded (as they are throughout this

analysis), this inner energy scale is equal to one; taking γ on the order of one would result in essentially no averaging at all. The outer energy scale $E_{\max}$ is the energy equal to $\hbar/T_{\min}$, where $T_{\min}$ is the shortest periodic orbit. For γ's larger than this energy, we are smoothing out secular variations, which we do not want to do. Therefore γ must be between these two values. We can obtain an estimate of $E_{\max}$ by looking at the Δ_3 statistic of the eigenvalues [36]: $E_{\max}$ is approximately the value $L_{\max}$ for which $\Delta_3(L)$ saturates. For our system, we find $20 \leq L_{\max} \leq 40$: at $L = 20$, $\Delta_3(L)$ begins to fall short of the prediction for chaotic systems, and at $L = 40$, the $\Delta_3(L)$ value saturates. The value of ν obtained from the fits did not vary significantly (less than 4% for the regular states, less than 1% for the other two classes) for $\gamma = 25, 30, 35$, so we will fix $\gamma = 30$ for all further computations.

As confirmation that the corner basis states were not unfolded correctly, we fit the components from the corner states alone, and found large γ dependence for the chaotic states ($0.54 < \nu < 0.64$) and the regular states ($0.07 < \nu < 0.12$). However, for the quasichaotic levels there was little dependence ($0.53 < \nu < 0.54$); the reason for this small variance is not understood.

Once the components were unfolded for fixed m_0 and Δm_{12}, we combined them together into one data set in order to obtain higher statistics than would otherwise be possible. That is, we combine together $\xi(m_0, \Delta m_{12}, \lambda, \gamma)$ for all m_0 and Δm_{12} (except for the corner states) in the same spirit as Haq, Pandey, and Bohigas, who combined the unfolded data from several different nuclei [16, 17]. For the eigenvectors with energies in the chaotic regime, this theoretically combines together components all chosen from the same distribution, given by Eq. (5). However, for the quasichaotic energies, the classical limit displays varying degrees of chaos, hence we would expect the components to be chosen from χ^2 distributions with different values of ν [Eq. (7)]. What is the resulting distribution in this case? Assuming that there are a range of ν values equally represented, the resulting probability is given by

$$P_{\nu\mathrm{av}}(y) = \frac{1}{\nu_2 - \nu_1} \int_{\nu_1}^{\nu_2} P_\nu(y) d\nu. \tag{16}$$

Numerical integration shows that the above distribution is a distribution close to a χ^2 distribution with $\nu = (\nu_2 - \nu_1)/2$. For example, with $\nu_1 = 0.5$ and $\nu_2 = 0.8$, the resulting distribution is visually indistinguishable (on the scale shown in Fig. 1) from the χ^2 distribution with $\nu = 0.65$. (These values were chosen because the chaotic volume in the quasichaotic region varies from 0.5 to 0.8 [41].)

Before histogramming any subset of data, half of that data is thrown out at random. This is done because the data are correlated, as mentioned in Sec. 2, but if we consider a subset of the data, the correlations become insignificant. The fraction one-half was chosen because for large, real, unitary matrices (i.e., symmetric orthogonal matrices) approximately half of the components are independent.

Before histogramming the components, we took the logarithm of the data:

$$z(m_0, \Delta m_{12}, \lambda; \gamma) = \log_{10} \xi(m_0, \Delta m_{12}, \lambda; \gamma) \; ; \tag{17}$$

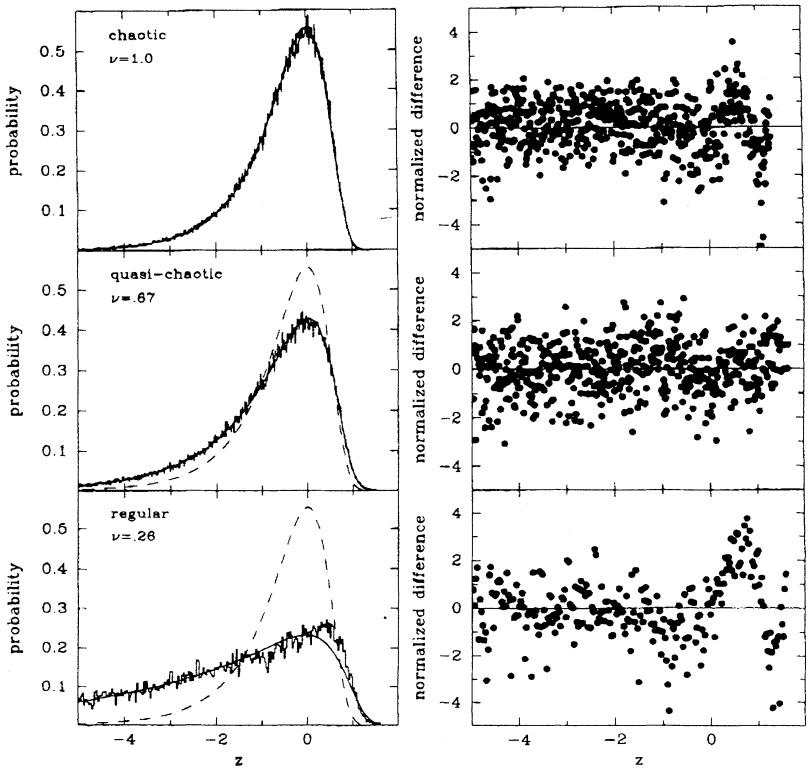

FIG. 1. The left column shows the histogrammed data for the different dynamics classes. The dashed line is the Porter-Thomas distribution [Eq. (5)]; the solid line is the best fit χ^2 distribution [Eq. (7)]; details of the fit are given in Table I. The right column is the corresponding normalized difference plot, i.e., the data minus the fit divided by the uncertainty. For the chaotic and regular data there are clear systematic deviations in the difference plot. (The data between $-6 < z < -5$ are left out for clarity. The fit in that regime is qualitatively similar to the fit between $-5 < z < -4$.)

TABLE I. Fit parameters for three different groupings (all eigenvectors and all components; scarred eigenvectors and all components; all eigenvectors and $I_0 = 0$ components) and three different classes (regular, quasichaotic, and chaotic). In all cases the corner components are omitted from the fit.

Class \ Parameter	Counts	Bins	ν	$\langle z \rangle$	B	χ^2	P_{fit}
			All levels				
chaotic	145796	600	1.000 ± 0.003	0.010 ± 0.002	0.996 ± 0.003	1.22	2×10^{-4}
quasichaotic	159052	600	0.666 ± 0.002	0.014 ± 0.002	1.004 ± 0.003	1.13	0.016
regular	21252	300	0.258 ± 0.003	-0.035 ± 0.008	1.087 ± 0.008	1.80	6×10^{-16}
			Scarred levels				
chaotic	14219	125	0.991 ± 0.010	-0.000 ± 0.005	0.992 ± 0.008	1.15	0.12
quasichaotic	10635	125	0.557 ± 0.008	-0.064 ± 0.008	0.998 ± 0.010	1.70	2×10^{-6}
			$I_0 = 0$ components				
chaotic	3091	60	0.907 ± 0.019	-0.017 ± 0.013	0.967 ± 0.018	1.96	2×10^{-5}
quasichaotic	3250	60	0.379 ± 0.011	-0.102 ± 0.018	1.028 ± 0.019	1.96	2×10^{-5}
regular	315	20	0.173 ± 0.034	0.000 ± 0.089	1.000 ± 0.012	19.0	0.0

this enlarges the scale near $\xi = 0$ where most of the counts are concentrated. The values of z were histogrammed for each dynamics class (regular, quasichaotic, and chaotic). We find the fit parameters were insensitive to the number of bins within a large range of bin values. Only the data with $z \geq -6$ were histogrammed; since the eigenvectors were calculated in single precision, components smaller than this were not reliably calculated. This cutoff excluded less than 1% of the data for the chaotic and quasichaotic data, and 6% of the data for the regular levels. The uncertainty in each bin was taken as the square root of the number of counts [42].

The resulting histogram was then fit to the distribution derived from the χ^2 distribution [Eq. (7)] for the variable $z = \log_{10} \xi = \log_{10}(y/\langle y \rangle)$. The program fits not only the value of ν, but also $\langle z \rangle$ and the normalization constant B. We expect $\langle z \rangle = 0$ (because $\langle \xi \rangle \approx 1$) and $B = 1$. Since this is a nonlinear fit, the value of ν is estimated using the maximum-entropy method [43], then fit parameters were calculated to minimize χ^2, using the Levenberg-Marquardt algorithms as implemented in Ref. [44]. (Note that name χ^2 refers to both the functional form fit [Eq. (7)] and the measure of goodness of fit; the reference should be clear from context.)

Because of the large number of counts (see Table I) we are able to be discriminating about the quality of fit. The quality was judged by three criteria: the value of χ^2 per degree of freedom, by the probability $P_{\text{fit}}(\chi^2)$ that χ^2 should be as large as it is [42], and by the trends in the normalized difference plot. This plot is the difference between the fit and the data, divided by the uncertainty; if the difference shows systematic deviations, the fit is questionable. The values of χ^2 and P_{fit} did depend on bin size and smoothing; χ^2 changed by as much as 16% and P_{fit} by five orders of magnitude for the chaotic data and two orders of magnitude for the quasichaotic data. (P_{fit} is much more sensitive to the errors than χ^2 [44].) Because the quality of fit varied significantly, in the next section we will show typical results, not the best results.

VI. RESULTS

The results for the three classes of classical dynamics are shown in Fig. 1; the fit parameters are in Table I. The values of ν are as expected. For the chaotic levels we obtain $\nu = 1.00$, which is exactly the Porter-Thomas prediction from RMT, for the quasichaotic levels $\nu = 0.667$, for the regular $\nu = 0.27$. There is no prediction for these last two values, but the trend is correct: ν is decreasing as the classical dynamics becomes more regular. In all cases $\langle z \rangle$ and B are near their expected values, although the parameters for the regular levels deviate the most.

Next we must consider the quality of fit. Only the fit for the quasichaotic levels gives confidence in the model; for the other two fits the probability P_{fit} is far too small to validate the model (acceptable values should be no smaller than 0.01), and the difference plots for the chaotic and regular levels show trends in the data not accounted for by the fit. In addition, the fit for the chaotic and regular levels does not improve if we take the cutoff to be 0.9 instead of 0.85, hence the unfolding procedure does not appear to be at fault.

However, a different perspective of the results may be taken. Given that the statistically significant deviations for the chaotic levels in Fig. 1 are at the 2% level or lower, we claim an accurate model of the components is given by the energy-smoothed behavior plus GOE fluctuations. This modeling of the components should be much quicker computationally than the exact solution of the Schrödinger equation in the semiclassical limit.

Now we turn to the scarred eigenstates. The 64 scarred states in the chaotic and quasichaotic range are chosen by picking those eigenvectors with scar strengths larger than 0.1 (where the scar strength is the total probability of an eigenvector along the $I_0 = 0$ line). All of these states could easily be picked out visually as scarred states, as can be seen in the left-hand column, Fig. 2. At these energies, almost all of the triangle is energetically accessible, except for the corners; therefore the strong localization

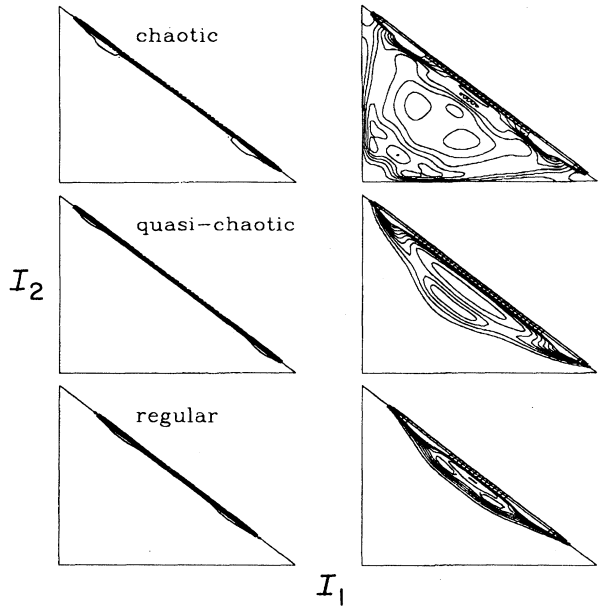

FIG. 2. The left column shows the Husimi projection of an eigenstate onto the action triangle (I_1 vs I_2), one for each dynamics class. Each eigenstate is clearly scarred by the $I_0 = 0$ periodic orbit (energy conservation keeps the wave functions only out of the corners of the triangle). It is important to note that there is no such thing as a scarred regular state since we expect localization on quantized tori. However, since there are states localized along the $I_0 = 0$ orbit in the regular region, we include one such state for comparison. The contours shown are the $10\%, 20\%, \ldots, 90\%$ of maximum contours; at this level all three look similar. However, in the right column we plot the $1\%, 2\%, \ldots, 9\%$ of maximum contours, and see that the decreasing degree of chaos of the classical limit leads to a stronger concentration on the periodic orbit.

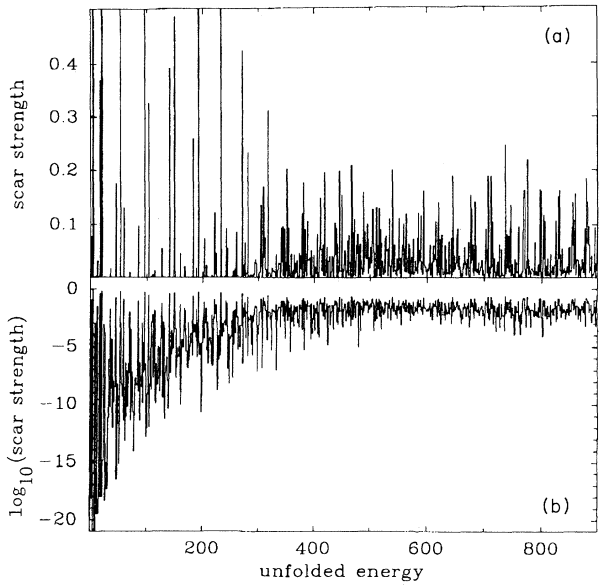

FIG. 3. The top plot shows the scar strength of each eigenvector (i.e., the total probability of that state along the $I_0 = 0$ periodic orbit) vs the unfolded eigenvalue (ε) of that state. The bottom plot shows the same on a logarithmic scale. It is clear that the distribution is more democratic for the chaotic states ($530 < \varepsilon < 891$) than for the quasichaotic ($126 < \varepsilon < 528$) and the regular states ($-1 < \varepsilon < 124$).

along one edge is remarkable. Note that this is a special case where no trajectories other than the periodic orbit can exist on that line; this makes for particularly clean scarring which is not expected in general.

The first indication that scarring depends on the global dynamics is seen in a plot of scar strength versus unfolded eigenvalue [Fig. 3(a)]. Since the energy is unfolded, the density of states is uniformly one. Therefore, in the region of low energy where there are few spikes, that indicates not a lack of states, but a lack of strength. This plot shows that there is clearly a difference in the distribution of strength among the states. For the low energies (which are regular) one or two states carry all the weight, and the distribution becomes more democratic as the energy increases and the system becomes more chaotic. This is emphasized in Fig. 3(b) where we plot the same values on a logarithmic scale.

By histogramming all the components of the scarred eigenstates alone, we can make this observation more quantitative. Here, we follow the same procedure as above, except we only look at the components of the eigenstates which are scarred by the $I_0 = 0$ periodic orbit. Part of the $I_0 = 0$ line is considered a corner and must be discarded. The choice of cutoff for $\langle \xi \rangle_{\text{energy}} = 0.85$ comes from this scarring region. If we take the cutoff as large as 0.9, then almost the entire $I_0 = 0$ line is discarded; if we take the 0.85 cutoff, more than half of the line is included; the other half of the line is visited only for energies near zero.

The results for the scarred states are also given in Table I and shown in Fig. 4. From the fit, we see that the scarred chaotic levels are consistent with the Porter-Thomas prediction, although there are trends in the difference plot. For the quasichaotic levels, the fit is qualitatively good, but again there are significant deviations from the fit. However, it is clear from the fit that the distribution for these levels is significantly less democratic than for the chaotic levels, just as for the nonscarred states. Therefore the fluctuations of even the scarred states can be modeled by Eq. (7).

To show how this difference is manifested in individual eigenstates we examine the Husimi distributions, i.e., the overlap of a fixed state with a coherent state [38, 40]:

$$W_\Psi(I_1, I_2, \theta_1, \theta_2) \equiv |\langle I_1, I_2, \theta_1, \theta_2 | \Psi \rangle|^2 \quad . \tag{18}$$

To more clearly see the scars, we plot not the Husimi distribution, but its projection onto action space:

$$P_{W,\Psi}(I_1, I_2) \equiv \int d\theta_1 \int d\theta_2 W_\Psi(I_1, I_2, \theta_1, \theta_2). \tag{19}$$

Figure 2 shows these projections for three states localized along the $I_0 = 0$ line, one in each dynamics class. On a plot showing the contours at $10\%, 20\%, \ldots, 90\%$ of the maximum value (left-hand column) they are very similar; however if we plot the contours $1\%, 2\%, \ldots, 9\%$ of the maximum (right-hand column), we see that the distribution off of the scarred orbit depends strongly on

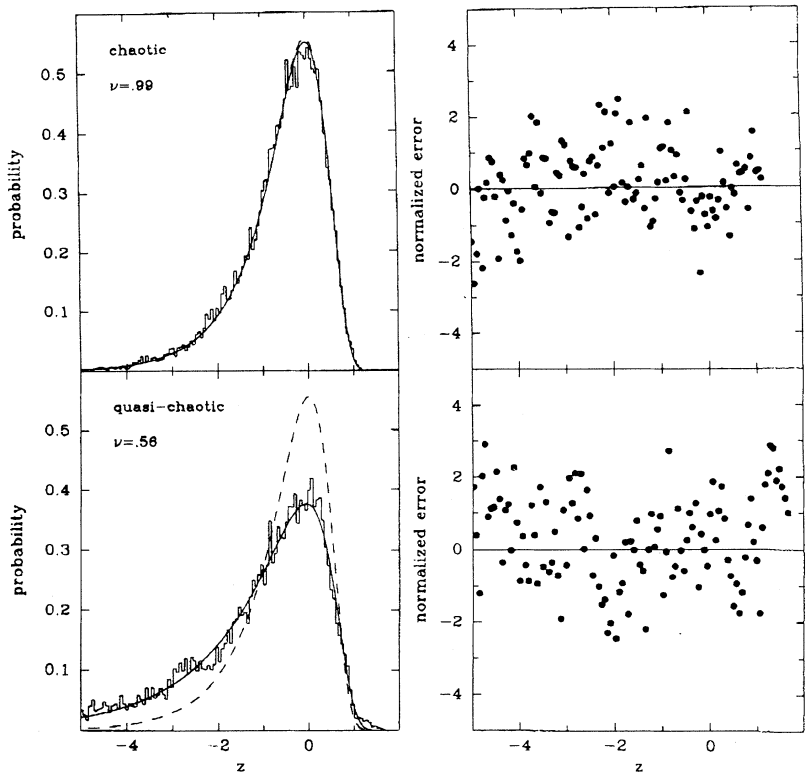

FIG. 4. Same as Fig. 1, except only the components from the scarred eigenvectors of each dynamics class are histogrammed, and the regular levels are omitted due to the small number of regular "scarred" states. In both cases there are clear systematic deviations in the difference plot.

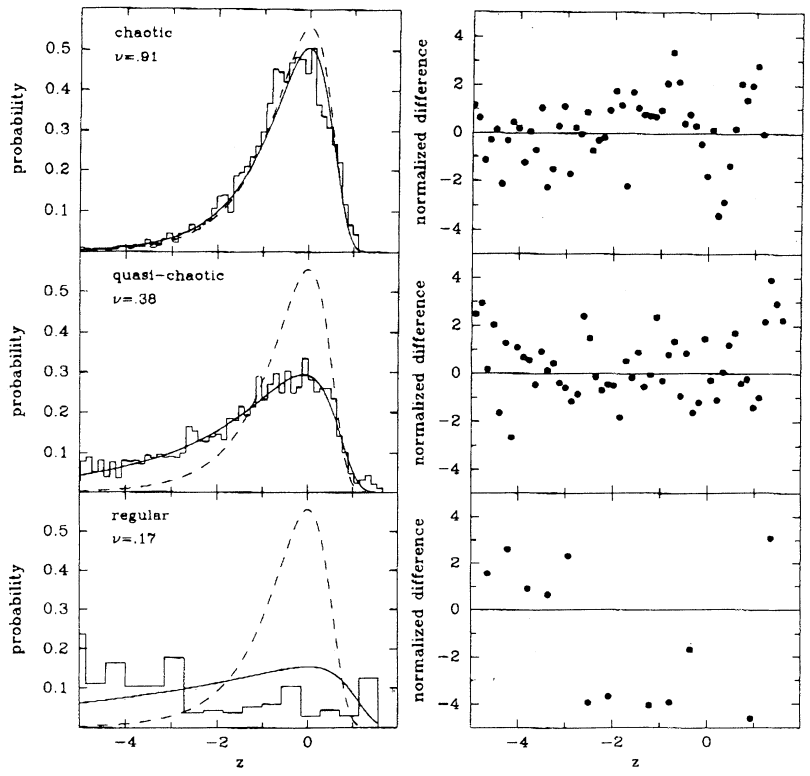

FIG. 5. Same as Fig. 1, except only the components along the $I_0 = 0$ line are histogrammed. In all cases there are clear systematic deviations in the difference plot.

the classical dynamics. We see clearly that the increased regularity in the classical dynamics gives rise to an increased localization along the periodic orbit. These differences have also been seen in the quantal surfaces of section [45].

We can also probe the effects of scarring by looking at the statistics of the components along the $I_0 = 0$ line (i.e., all components with $m_0 = 0$) for all eigenvectors. These results are in Table I and shown in Fig. 5. Here the values for ν are less than expected from the fits in Fig. 1, and the difference plots show trends not accounted for by the fit. These deficiencies are likely due to the unfolding: all of these $m_0 = 0$ components give $0.85 < \langle \xi \rangle < 0.9$, so the unfolding is only marginally acceptable. However, the trends are clear; the sharing of strength becomes less democratic as the dynamics becomes more regular.

VII. CONCLUSIONS

We have fit the fluctuations of unfolded components to a χ^2 probability distribution for ν degrees of freedom, with ν decreasing from 1 as the classical dynamics becomes more regular. The high statistics allow us to say that the fit is qualitative at best since there are statistically significant deviations between experiment and theory. However, the level of agreement is good enough to claim that the fluctuations are modeled accurately by a χ^2 distribution with ν degrees of freedom. We emphasize that correct unfolding of the data is essential, although in the special (but common) case of two degrees of freedom kinetic plus potential Hamiltonians, this is not necessary.

Our greatest interest is the interplay between scarring by periodic orbits (which are particular to the system) and the statistics of the component fluctuations (which are proposed to be universal). We find that there is no incompatibility between these two; this idea has been suggested before by Heller, O'Connor, and Gehlen [46] and Aurich and Steiner [33]. On the contrary, the distribution of the fluctuation gives enough freedom for the eigenvectors to cluster the large probabilities along periodic orbits. However, we believe it is incorrect to conclude that scars are always merely chance occurrences, since the energy-averaged strength peaks at energies which quantize the action of the periodic orbit, and there is a strong localization along the stable and unstable manifold in phase space [40].

In this light, we find that POT and RMT are complementary semiclassical theories. POT tell us that there can be enhanced probability near the short periodic orbits and that the strength of scarring depends on the stability of that orbit (or, from the work of Frisk [47], the Kolmogorov-Sinai entropy); RMT tells us that the degree of chaos in the classical dynamics determines the strength off of the periodic orbit of a single scarred eigenstate as well as the distribution of scarring strength among neighboring eigenvectors. These relatively new intuitions have not come directly from our classical intuition, but have grown out of work in the semiclassical regime of quantum mechanics.

ACKNOWLEDGMENTS

The author gratefully acknowledges useful discussions with Y. Alhassid, programming by L. Janoo, the support of the Roland H. O'Neal Fund, and the National Science Foundation under Grant No. PHY-9009769, as well as computer time on the CRAY X-MP provided by the San Diego Supercomputing Center.

[1] M. V. Berry, in *Chaotic Behavior of Deterministic Systems*, edited by G. Iooss, R. G. H. Helleman, and R. Stora (North-Holland, Amsterdam, 1983).
[2] M. Tabor, *Chaos and Integrability in Nonlinear Dynamics* (Wiley, New York, 1989).
[3] C. L. Siegel, Math. Ann. **128**, 144 (1954); Ann. Math. **42**, 806 (1941).
[4] M. C. Gutzwiller, J. Math. Phys. **8**, 1979 (1967); **10**, 1004 (1969); **11**, 1791 (1970); **12**, 343 (1971).
[5] R. Balian and C. Bloch, Ann. Phys. (N.Y.) **69**, 76 (1972).
[6] M. V. Berry, Proc. R. Soc. London. Ser. A **423**, 219 (1989).
[7] E. B. Bogomolny, Physica D **31**, 169 (1988).
[8] M. C. Gutzwiller, *Chaos in Classical and Quantum Mechanics* (Springer-Verlag, New York, 1990).
[9] E. J. Heller, Phys. Rev. Lett. **53**, 1515 (1984).
[10] M. L. Du and J. B. Delos, Phys. Rev. A **38**, 1896 (1988); **38**, 1913 (1988).
[11] F. J. Dyson, J. Math. Phys. **3**, 140 (1962).
[12] M. L. Mehta, *Random Matrices* (Academic, New York, 1991).
[13] C. E. Porter, *Statistical Theories of Spectra: Fluctuations* (Academic, New York, 1965).
[14] T. A. Brody, J. Flores, J. B. French, P. A. Mello, A. Pandey, and S. S. M. Wong, Rev. Mod. Phys. **53**, 385 (1981).
[15] O. Bohigas and M.-J. Giannoni, in *Mathematical and Computational Methods in Nuclear Physics*, edited by J. S. Dehesa, J. M. G. Gomez, and A. Polls (Springer-Verlag, Berlin, 1983).
[16] R. U. Haq, A. Pandey, and O. Bohigas, Phys. Rev. Lett. **48**, 1086 (1982).
[17] O. Bohigas, R. U. Haq, and A. Pandey, Phys. Rev. Lett **54**, 1645 (1985).
[18] O. Bohigas, M.-J. Giannoni, and C. Schmit, Phys. Rev. Lett. **52**, 1 (1984).
[19] B. Eckhardt, Phys. Rep. **163**, 205 (1988), and references therein.
[20] M. V. Berry, Proc. R. Soc. London. Ser. A **400**, 229 (1985).
[21] R. Balian, Nuovo Cimento B **57**, 183 (1968).
[22] Y. Alhassid and R. D. Levine, Phys. Rev. Lett. **57**, 2879 (1986).
[23] Y. Alhassid and M. Feingold, Phys. Rev. A **39**, 374 (1989).
[24] H. I. Liou, H. S. Camarada, S. Wynchank, M. Slagowitz, G. Hacken, F. Rahn, and J. Rainwater, Phys. Rev. C **5**, 974 (1972).
[25] G. E. Mitchell, E. G. Bilpuch, J. F. Shriner, Jr., and A. M. Lane, Phys. Rep. **117**, 1 (1985).

[26] J. P. Draayer, J. B. French, and S. S. M. Wong, Ann. Phys. (N.Y.) **106**, 472 (1977).
[27] R. Chrien, Phys. Rep. **64**, 337 (1980).
[28] Y. Alhassid, A. Novoselsky, and N. Whelan, Phys. Rev. Lett. **65**, 2971 (1990); Y. Alhassid and N. Whelan, *ibid.* **67**, 816 (1991).
[29] P. Šeba, Phys. Rev. Lett. **64**, 1855 (1990).
[30] S. W. McDonald and A. N. Kaufman, Phys. Rev. A **37**, 3067 (1988).
[31] M. Shapiro and G. Goelman, Phys. Rev. Lett. **53**, 1714 (1984).
[32] F. M. Israliev, Phys. Rev. Lett. A **125**, 250 (1987).
[33] R. Aurich and F. Steiner, Physica D **48**, 445 (1991).
[34] H. J. Lipkin, M. Meshkov, and A. J. Glick, Nucl. Phys. **62**, 188 (1965).
[35] S. Y. Li, A. Klein, and R. M. Dreizler, J. Math. Phys. **11**, 975 (1970).
[36] D. C. Meredith, S. E. Koonin, and M. R. Zirnbauer, Phys. Rev. A **37**, 3499 (1988).
[37] A. Perelomov, *Generalized Coherent States* (Springer-Verlag, Berlin, 1986); W.-M. Zhang, D. H. Feng, and R. Gilmore, Rev. Mod. Phys. **62**, 867 (1990); J. Kurchan, P. Leboeuf, and M. Saraceno, Phys. Rev. A **40**, 6800 (1989); L. G. Yaffe, Rev. Mod. Phys. **54**, 407 (1982).
[38] P. Leboeuf and M. Saraceno, J. Phys. A **23**, 1745 (1990).
[39] P. Leboeuf and M. Saraceno, Phys. Rev. A **41**, 4614 (1990).
[40] P. Leboeuf, D. C. Meredith, and M. Saraceno, Ann. Phys. (N.Y.) **208**, 333 (1991).
[41] D. C. Meredith, Ph.D. thesis, California Institute of Technology, 1987 (unpublished); available from University Microfilms, Ann Arbor, MI 48106.
[42] P. R. Bevington, *Data Reduction and Error Analysis for the Physical Sciences* (McGraw Hill, New York, 1969).
[43] Y. Alhassid, N. Agmon, and R. D. Levine, Chem. Phys. Lett. **53**, 22 (1978).
[44] W. H. Press, B. P. Flannery, S. A. Teukolsky, and W. T. Vetterling, *Numerical Recipes* (Cambridge University Press, Cambridge, 1986).
[45] D. C. Meredith, J. Stat. Phys. **68**, 97 (1992).
[46] E. J. Heller, P. W. O'Connor, and J. Gehlen, Phys. Scr. **40**, 354 (1989).
[47] H. Frisk, Phys. Scr. **43**, 545 (1991).